Stellar Kinematics in the Inner Spheroid of Andromeda:

Discovery of Substructure Along the SE Minor Axis and its Relationship to the Giant Southern Stream

K. M. Gilbert[1], M. Fardal[2], J. S. Kalirai[1], P. Guhathakurta[1], M. C. Geha[3], J. Isler[4], S. R. Majewski[6], J. C. Ostheimer[6], R. J. Patterson[6], D. B. Reitzel[5], E. Kirby[1], M. C. Cooper[7]

Evidence and Properties of Substructure

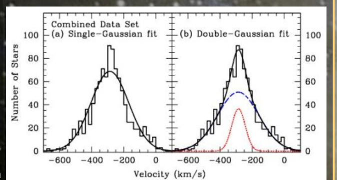

Figure 2: A kinematically cold population is observed in the M31 RGB velocity distribution. The line of sight velocity distribution of our M31 RGB sample. The data is inconsistent with the maximum-likelihood single Gaussian fit (a χ^2 test returns P«1%). The distribution is well-fit by a sum of 2 Gaussians: a kinematically hot component, which is the underlying inner spheroid of M31 (blue dashed curve, σ_{sph}=128.9 km s^{-1}), and a kinematically cold component (red dotted curve, σ_{sub}=42.2 km s^{-1}) which comprises 19% of the total population. Stars were identified as M31 red giants using the diagnostic method of Gilbert et al. (2006), *without using radial velocity*.

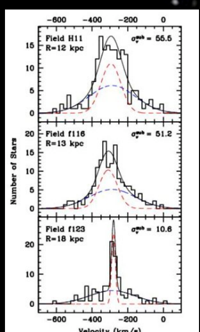

Figure 3: The velocity dispersion of the substructure decreases with increasing radial distance from M31. The line of sight velocity distribution of M31 RGB stars in the 3 fields in which the kinematically cold component is clearly detected, with the best double-Gaussian fit to each field (black solid curves). The velocity dispersion of the cold component (red dashed curves) decreases with increasing radial distance (also shown in Fig. 6). The hot component (blue dashed curves) was held fixed at the best-fit values from the fit to the combined data set (Fig. 2). The cold component comprises 44% of the population in fields H11 and f116, and 31% of the population in field f123. Not shown: the individual fields without detected substructure show no sign of a decreasing *spheroid* velocity dispersion with radius (out to R_{proj} = 30 kpc).

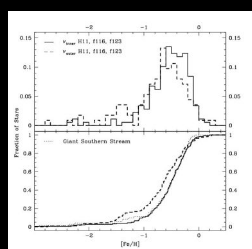

Figure 3: The stars associated with the cold component are more metal-rich than the M31 spheroid stars. The [Fe/H] distribution of stars with velocities within ±1σ (v_{inner}) and outside ±2σ (v_{outer}) of the mean velocity of the cold component in the three fields in which it is observed. The v_{inner} (substructure) [Fe/H] distribution is highly contaminated (32.5%) by spheroid stars. The v_{outer} (spheroid) [Fe/H] distribution has minimal contamination from the substructure. After accounting for the effects of spheroid contamination, the mean [Fe/H] of the substructure is ~ 0.2 dex more metal-rich than the mean [Fe/H] of the spheroid ($\langle Fe/H \rangle_{sub}$= -0.52, $\langle Fe/H \rangle_{sph}$= -0.72).

THE DISRUPTION OF A DWARF GALAXY: Debris in the form of coherent shells is observed in many elliptical galaxies, and is believed to be formed by the disruption of a satellite galaxy on a nearly radial orbit. Fardal et al. 2007 postulate that the NE and Western "shelves" observed in Andromeda are a similar phenomenon, and have been created by the progenitor of the giant southern stream (Fig. 1). They simulate the interaction of a dwarf galaxy with Andromeda, with the satellite's orbit chosen to reproduce the observations of the giant southern stream and the NE shelf. This orbit also reproduces the Western shelf, and *predicts a fourth, faint shell on the eastern side of the galaxy* (Fig. 5) which would be the most visible in the southeast. This fourth "southeast shelf" would be the *furthest forward continuation of the giant southern stream*.

DISCOVERY OF SUBSTRUCTURE: Using spectra of Andromeda red giant branch stars obtained with the DEIMOS spectrograph on the Keck II 10-m telescope (Fig. 1), we have ***discovered a kinematically cold component along the southeast minor-axis of Andromeda with the same spatial and kinematical properties as the southeast shelf predicted in the Fardal et al. (2007) simulations*** (Figs. 2-6). The most likely explanation for the SE minor-axis substructure is that it is the forward continuation of the giant southern stream. As such, it will add significant observational constraints to the existing observations, and will *enable detailed modeling of Andromeda's mass distribution*. It also sheds light on the discovery of a significant intermediate-age population at 12 kpc along the SE minor axis (field H11, Brown et al. 2003) and the remarkable similarity in the ages and metallicities of stars in this "spheroid" field and a field on the giant southern stream (Brown et al. 2006).

Location of Fields

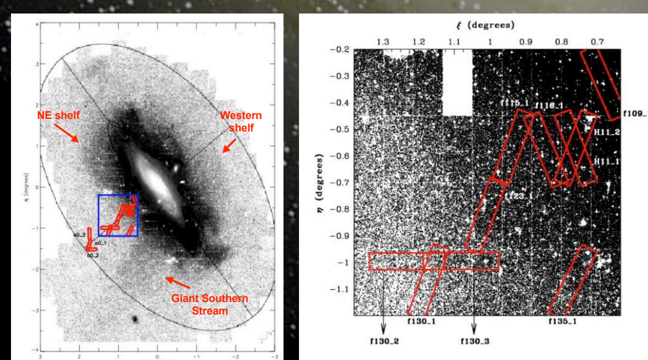

Figure 1: Positions and orientations of the Keck/DEIMOS spectroscopic masks. These two figures show the locations of the fields used in this analysis, which span a range in projected radial distance of 9 to 30 kpc from the center of M31. *Left*: The location and orientation of each of the Keck/DEIMOS masks (red rectangles) superimposed on a starcount map of M31 from Ibata et al. (2005). The blue square represents the size and position of the CFHT/MegaCam image used to design the majority of the masks. *Right*: A starcount map of the CFHT/Megacam image, with the location and orientation of the Keck/DEIMOS masks marked as red rectangles. There is an apparent edge in the density of star counts in the image, running from the upper left to the lower right. This is likely the edge of the predicted "southeast shelf" (Fardal et al. 2007).

Relationship to the Giant Southern Stream

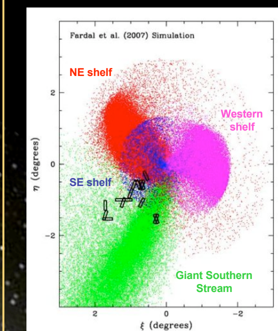

Figure 5: The spatial distribution of fields with observed substructure matches the spatial location of the predicted southeast shelf (blue particles). The location of our Keck/DEIMOS masks, superimposed on a map of the particles in the Fardal et al. 2007 simulations, in standard M31-centric coordinates. Particles approaching their first pericentric passage form the giant southern stream (green). Particles approaching their second pericentric passage form the NE shelf (red). Particles on their third pericentric passage form the Western shelf (magenta). These three features can be seen in the M31 star count map in Fig. 1 (Ibata et al. 2005). Particles on their fourth pericentric passage form the predicted southeast shelf (blue). The edge of this feature passes through fields f123 and f135, and is a good match to the edge observed in the CFHT/MegaCam star count map in Fig. 1.

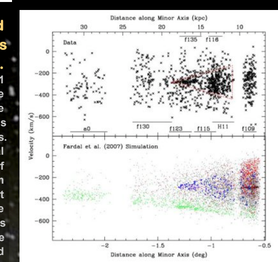

Figure 6: The shape of the observed substructure in the R_{proj}–v_{los} plane is a classic feature of a shell system. *Top*: The line of sight velocity distribution of M31 RGB stars as a function of distance along the minor axis. The substructure forms a distinctive triangular shape in the R_{proj}–v_{los} plane, which is the signature of a shell system. *Bottom*: v_{los} vs. minor axis distance for particles from the Fardal et al. 2007 simulation of the merger of a dwarf galaxy with M31. Green particles are debris from the giant southern stream, red particles are part of the NE shelf, blue particles are part of the predicted "southeast shelf," and black particles are from the bulge+disk+stellar-halo of M31. The distribution of southeast shelf particles is a good match with the observed substructure.

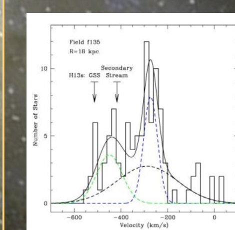

Figure 7: The velocity distribution of field f135 is consistent with at least 2 cold populations. Field f135 is inconsistent with being drawn from either a single or double Gaussian. The simulations predict that this field should have significant contamination from the giant southern stream, as well as the southeast shelf. A triple Gaussian is a good fit to the data, consisting of M31's underlying spheroid (black dashed curve), the southeast shelf (blue dashed curve), and (potentially) the giant southern stream (green dashed curve). The width of the most negative component is significantly wider (σ=55 km s^{-1}) than other observations of the giant southern stream. Kalirai et al. 2006 found two cold components in a field at a similar radial distance as f135 along the giant southern stream (H13s); the location and width of the two components from H13s are shown as arrows and horizontal lines.

REFERENCES

- Brown et al. 2003, ApJ, 592, L17
- Brown et al. 2006, ApJ, 636, L89
- Fardal et al. 2007, MNRAS, in press (astro-ph/0609050)
- Gilbert et al. 2006, ApJ, 652, 1188
- Ibata et al. 2005, ApJ, 634, 287
- Kalirai et al. 2006, ApJ, 641, 268

This poster is based on work presented in Gilbert et al. 2007, ApJ, in press (astro-ph/0703029)

Presented at the Milky Way Halo Conf., Bonn, 2007, Poster #31

AFFILIATIONS:

1) University of California, Santa Cruz
2) University of Massachusetts, Amherst
3) NRC Herzberg Institute of Astrophysics
4) Fisk University/Vanderbilt University, visiting student, UCSC
5) University of California, Los Angeles
6) University of Virginia
7) University of California, Berkeley

ACKNOWLEDGEMENTS

- This research was supported in part by NSF grants AST-0307966 and AST-0507483 and NASA/STScI grants GO-10265.02 and GO-10134.02 (P. G., K.M.G., and J.S.K.)
- We are grateful to Mike Rich for his role in the acquisition of many of the Keck/DEIMOS masks.
- The spectra were obtained using DEIMOS at the W.M. Keck Observatory, which is operated as a scientific partnership among the California Institute of Technology, the University of California, and NASA, and was designed and built at the University of California at Santa Cruz (PI: S. Faber)
- The imaging data was obtained using the (1) MOSAIC camera at Kitt Peak National Observatory of the National Optical Astronomy Observatories, which is operated by AURA, Inc., under cooperative agreement with the NSF; and (2) MegaCam on the Canada-France-Hawaii telescope, which is operated by NRC (Canada), CNRS (France), and the University of Hawaii
- The spectroscopic data reduction was carried out using the *spec2d* and *spec1d* software pipelines developed by the DEEP2 team at the University of California, Berkeley